Solar Energy Materials & Solar Cells 120 (2014) 275–281

Contents lists available at ScienceDirect

Solar Energy Materials & Solar Cells

journal homepage: www.elsevier.com/locate/solmat

On the origin and formation of large defect clusters in multicrystalline silicon solar cells

Dietmar Kohler*, Annika Zuschlag, Giso Hahn

University of Konstanz, Department of Physics, P.O. Box X916, 78457 Konstanz, Germany

ARTICLE INFO

Article history:
Received 10 July 2013
Received in revised form
12 September 2013
Accepted 13 September 2013
Available online 10 October 2013

Keywords:
Multicrystalline silicon
Solar cell
Defect cluster
Luminescence
Crystal orientation
Raman

ABSTRACT

Large defect clusters can represent a serious reduction of the material quality of multicrystalline silicon and the efficiency of the resulting solar cells. It is useful to find the origin of these defect-rich regions in order to understand their formations. For this work, multicrystalline silicon wafers from different positions of a compensated p-type silicon brick were processed to solar cells with a homogeneous emitter and screen-printed metallization. The solar cells from the main part of the brick showed efficiencies between 15.6% and 16.1%. The characterization for this work focuses on the positions of the three largest defect clusters by means of detailed optical, crystal orientation and electrical loss measurements. This allows the localization of the defect clusters' origins during crystallization. The locations where the observed defect clusters started to grow, show similar crystal configurations. This implies that the large clusters formed preferentially at grain boundaries between specific grain orientations. A smaller cluster disappeared at a grain boundary. The characterization showed the same crystal configuration as for the three large growing clusters.

1. Introduction

Defect clusters are local accumulations of crystal defects like grain boundaries and especially dislocations. They can heavily decrease the material quality by drastically reducing the diffusion length of minority charge carriers. The influence of dislocations on the material quality and on solar cells depends on several factors, e.g. their decoration with impurities [1–4]. The reduction of the diffusion length for an increasing dislocation density was modeled by Donolato [5]. On the basis of Donolato's work, Kieliba et al. [6] studied the decrease of the open circuit voltage V_{oc} for increasing dislocation densities. In an earlier work, we showed that this applies also for defect clusters [7]. Experiments on small solar cells have been presented, which were cut out of large area cells that included extended defect clusters. The small cells that contained defect clusters showed lower V_{oc} and lower short circuit current densites j_{sc} than dislocation-free solar cells. These effects were caused by defect clusters as well as by large networks of dislocations. Haunschild et al. [8] presented a direct correlation between V_{oc} and the fraction of crystal defects, which had been calculated from photoluminescence (PL) images.

Dislocations are typically caused by stresses within the crystal. These can be mechanical or thermal gradients occurring during crystallization of the ingot or during processing. Häßler et al. [9] stated from numerical simulations that the dislocation density during crystallization follows three phases. A first strong dislocation generation right after the solidification is expected. This is followed by a dislocation multiplication during cooling down to 600 °C. Below this temperature, the dislocation multiplication stops. Usami et al. [10] concluded from their comparisons of shear stress calculations with dislocation density measurements that the dislocation densities in multicrystalline silicon are related to the shear stresses around grain boundaries. On the other hand, it also seems to be possible to reduce dislocations by small stresses. Hartman et al. [11] observed significant decreases of the dislocation densities in SiN_x coated String Ribbon multicrystalline silicon wafers that were annealed at temperatures of up to 1366 °C for 6 h. According to works of Di Sabatino and Stokkan, it is also possible to achieve higher grain sizes as well as preferred grain orientations for increased initial ingot cooling rates [12].

Grain boundaries between two neighboring grains can be classified according to the crystal configurations and symmetries. Boundaries of grains that share a regular part of their atoms, are called coincidence site lattice (CSL) boundaries. They are classified by Σ, which is the reciprocal density of coincidence sites. Boundaries with high symmetries appear more often due to lower formation energies. CSL boundaries with increased degrees of symmetry are twin boundaries. The highest fraction of common atoms represents Σ3 grain boundaries where every third atom is part of both crystal grains. Examples for different twin boundaries will be presented in the results.

This present work has the purpose to focus on the origin and the formation of similar large defect clusters. Several hundred wafers from the same brick were available for this experiment.

* Corresponding author. Tel.: +49 7531 88 3174; fax: +49 7531 88 3895.
E-mail address: dietmar.kohler@uni-konstanz.de (D. Kohler).

0927-0248/$ - see front matter © 2013 Elsevier B.V. All rights reserved.
http://dx.doi.org/10.1016/j.solmat.2013.09.018

Some of the wafers were processed to solar cells and were measured using a forward biased electroluminescence (EL) setup. This enables us to identify the lateral and vertical positions of several clusters' origins. This information can be used for detailed measurements at these sections. The parts of neighboring wafers that contain the cluster formation areas were cut into 2×2 cm^2 pieces. After a polishing etch, the positions of the cluster origins were scanned using the EBSD (electron backscatter diffraction) mode of a scanning electron microscope (SEM) to receive information about the crystal orientation. From the crystal orientation of two neighboring grains, the grain boundary types can be calculated if the boundaries are specific CSL boundaries.

Other neighboring wafers were etched in a grain-selective or a dislocation-selective solution. The etched wafers were investigated with an optical microscope or scanned using an optical scanner setup to receive optical information about the crystal structure and the dislocation formations. This allows to investigate and to compare the crystal structures at the origins of the largest defect clusters.

2. Materials and experiment

The studied material was part of the center brick of a compensated p-type multicrystalline silicon ingot that was sawn into 25 bricks. Compensated silicon typically contains higher concentrations of boron and phosphorus as dopants. This is due to the different cleaning process. Furthermore, the net dopant concentration must be adjusted by the addition of boron or phosphorus because it is related to the bulk resistivity. The increased density of impurity atoms represents point defects that can also lead to higher dislocation densities. This may result in more defect clusters. These defects are not limited to compensated silicon, but are also well known in uncompensated multicrystalline silicon from conventional cleaning processes. The occurence of dislocations can be reduced by an adjusted cooling rate during the crystallization process, but not avoided completely [13,14].

For this experiment, 12.5×12.5 cm^2 wafers with a thickness of approx. 190 μm have been used. The wafers were taken from different heights of the same brick. All wafers from the wafered p-type part were numbered from the bottom to the top. These numbers are in the following indicated by "#". About half of the 500 wafers of this brick were available. 40 of these wafers were processed to solar cells with a homogeneous emitter formed by $POCl_3$ diffusion and screen-printed firing through SiN_x metallization. In a first step, the entire areas of all processed solar cells were characterized with an EL setup under forward and reverse bias. For selected cluster-containing parts of these solar cells, the spatially resolved internal quantum efficiency (IQE) was measured using light beam induced current (LBIC).

Neighboring wafers at these positions were either alkaline etched in order to enhance the reflection contrast between crystal grains of different orientations, or Secco etched [15] to reveal the dislocation structures. Further neighboring wafers at cluster containing areas were prepared for EBSD measurements. For that, the relevant sections were sawn out and chemical polishing (CP) etched with an etching solution based on hydrofluoric acid, acetic acid and nitric acid. The etched wafers were measured using a SEM with an included EBSD setup. Here, the sample is placed in an angle of 70°. Back-scattered electrons at the crystal planes lead to Kikuchi diffraction patterns. These patterns offer information on the crystal symmetries and the relative angles in between the grains. The orientations of crystal grains as well as the grain boundary types can be calculated using this information [16,17]. The orientation maps are based on inverse pole figures (IPF). In the shown EBSD maps, they are superposed with the grain boundary type lines according to the CSL. Additionally, Raman measurements, which are related to local stresses, were taken at one significant wafer area with a Raman setup by WITec using a HeNe laser with a wavelength of 633 nm.

3. Results

In the following, the current–voltage characteristic curves are shown in dependence of the ingot height. Then, we focus on the largest observed defect clusters in order to understand their formation mechanisms. Additionally, these results are compared to the opposite effect: a small defect cluster shrinks during the crystallization and is positioned in the opposite crystal configuration than the observed growing clusters.

3.1. Solar cell results

The solar cell results reveal typical limitations of compensated material. The current–voltage (I–V) characterization of the processed solar cells is shown in Fig. 1. The compensation of the segregating dopants leads to a decreasing net dopant concentration. This results in an increasing bulk resistivity towards the type inversion and limits V_{oc} as well as the efficiency. For an older material, we had observed an increasing j_{sc} in the upper part of the brick where the resistivity increases strongly [18]. We had assumed that the recombination losses at dopants might be reduced by the possible formation of B–P-pairs [19]. This was not observed for the new material, shown in Fig. 1 on the right. In

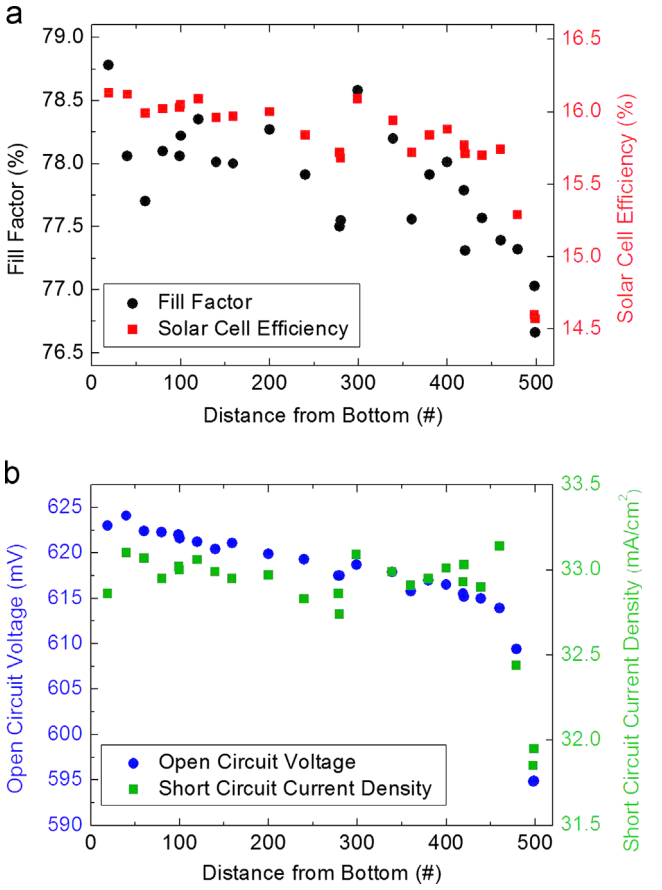

Fig. 1. I–V characterization in dependence of the distance from the position of the lowest wafer in the block according to the wafer number. The segregation and compensation of the dopants boron and phosphorus limit V_{oc}. In the upper part, j_{sc} decreases, probably due to losses that are caused by the high impurity concentrations. Minor problems in the solar cell process lead to the relatively strong scatter of the fill factor.